The following scientific article was officially published in the journal *IEEE Transactions on Biomedical Engineering*. This article's citation is as follows:

Adankon, Mathias M., Najat Chihab, Jean Dansereau, Hubert Labelle, and Farida Cheriet. "Scoliosis Follow-Up Using Noninvasive Trunk Surface Acquisition." IEEE Transactions on Biomedical Engineering, Vol. 60, no. 8 (2013): pp. 2262-2270.

doi: 10.1109/TBME.2013.2251466

The manuscript, as accepted by the publisher, is reproduced in the following pages.

Scoliosis Follow-Up Using Non-Invasive Trunk Surface Acquisition.

Mathias M. Adankon, Najat Chihab, Jean Dansereau, Hubert Labelle and Farida Cheriet

***Abstract*—Adolescent Idiopathic Scoliosis (AIS) is a musculoskeletal pathology. It is a complex spinal curvature in three-dimensional space that also affects the appearance of the trunk. The clinical follow-up of AIS is decisive for its management. Currently, the Cobb angle, which is measured from full spine radiography, is the most common indicator of scoliosis progression. However, cumulative exposure to X-rays radiation increases the risk for certain cancers. Thus, a non-invasive method for the identification of scoliosis progression from trunk shape analysis would be helpful. In this study, a statistical model is built from a set of healthy subjects using Independent Component Analysis (ICA) and Genetic Algorithm (GA). Based on this model, a representation of each scoliotic trunk from a set of AIS patients is computed and the difference between two successive acquisitions is used to determine if the scoliosis has progressed or not. This study was conducted on 58 subjects comprising 28 healthy subjects and 30 AIS patients who had trunk surface acquisitions in upright standing posture. The model detects 93% of the progressive cases and 80% of the non-progressive cases. Thus, the rate of false negatives, representing the proportion of undetected progressions, is very low, only 7%. This study shows that it is possible to perform a scoliotic patient's follow-up using 3D trunk image analysis, which is based on a non-invasive acquisition technique.**

***Index Terms*—Scoliosis, Independent Component Analysis, Genetic Algorithm, Surface topography, 3D trunk modeling, Pattern recognition.**

I. Introduction

Adolescent Idiopathic Scoliosis (AIS) is a deformity of the spine that is outwardly manifested by asymmetry and deformities of the external surface of the trunk. It consists of a complex spinal curvature in three-dimensional space: inclination in the frontal plane, rotation of vertebrae in the axial plane and modification of the natural curves in the sagittal plane. This pathology is often outwardly visible, but it may go unnoticed during its development for several years. Among patients with AIS, 1 in 25 cases have mild deformities and only 1 in 200 adolescents have deformities that progress to require either bracing or surgical treatment. In fact, the treatment decision is taken by the orthopedic doctor based on the progression of the scoliotic curve. Thus, it is important to know if and when the curve will progress in order to perform optimal treatment.

The Cobb angle is the gold standard for the monitoring and treatment decision of scoliosis. Several researchers consider that an increase in the Cobb angle measured from full spine radiography is the most common indicator of progression. On the other hand, there is as yet no reliable way to predict which deformities will progress; these patients are monitored with a series of X-rays acquired semi-annually during rapid adolescent growth. However, cumulative exposure to X-rays radiation significantly increases the risk for certain cancers [14].

Thus, during the last 30 years, many optical non-invasive surface measurement systems have been developed based on a 3D reconstruction of the back or of the whole trunk using various techniques: Moiré contour topography [40, 42], Integrated Shape Imaging System (ISIS)[43] and Quantec scanner [16, 32]. However, most studies have been focused on how to find the relationship between the Cobb angle and the indices computed from the trunk surface. Many research teams have tried to establish the correlation between the Cobb angle and various indices of torso asymmetry but their results are mitigated [2, 27, 28].

Recently, a few studies have addressed the issue of scoliosis progression using non-invasive acquisition. In [35], the authors have identified the best surface topography parameters correlated with scoliosis progression. Their results reveal that the most important measures are decompensation, trunk rotation and lordosis angle. In addition, Seze and Korvin [13] have presented a preliminary work on the feasibility of scoliosis follow-up using surface topography. This study used the Moiré contour topography technique, where the progression was assessed by looking at the rib hump, lordosis and spinal curve and by subjective comparison of the fringe mappings. However, the results are moderate: sensitivity 90% and specificity 60%.

In several previous studies, cross-sectional surface measurements have been proposed for noninvasive assessment of AIS trunk deformity. A drawback of these studies is that only the maximum index values along the trunk are used for monitoring AIS progression. To address that, Seoud and al [38] have proposed multilevel analysis using functional indices computed along the entire trunk. However, local

This work was supported by the GRSTB, the MENTOR program and the CIHR (Canadian Institutes of Health Research).

Mathias Adankon, Najat Chihab, Jean Dansereau and Farida Cheriet are with Ecole Polytechnique de Montreal, Montreal, Canada. (email: mathias-mahouzonsou.adankon@polymtl.ca, jean.dansereau@polymtl.ca, farida.cheriet@polymtl.ca).

Hubert Labelle and Stefan Parent are with Sainte-Justine Hospital Research Center, Montreal, Canada (email: hubert.labelle@recherche-ste-justine.qc.ca, stefan.parent@umontreal.ca).

Manuscript received September 15, 2012.

trunk deformations such as asymmetry of the shoulders, waist or scapulae cannot been characterized by these functional indices. Thus, in our recent work [1], we have proposed a method for analyzing scoliotic trunk deformities using Independent Component Analysis (ICA), and have shown that the independent components capture the local scoliosis deformations.

ICA is a statistical method that attempts to express the observed data with a linear combination of mutually independent variables [12]. ICA finds the independent components, also called sources, by maximizing the statistical independence between the estimated components. ICA was originally developed to deal with the blind source separation problem. With the recent increase of interest in ICA, various applications have been designed based on this statistical technique. Among them, we have feature extraction or data representation, which consists of computing a small vector representation of data (sound, image, etc) [23, 31, 5].

Recently, ICA has been used for image segmentation [30] and medical image analysis [8, 19, 41]. Boquete et al. [8] have proposed a thermographic image analysis based on ICA for automated detection of high tumor risk areas. Hassen et al [19] used ICA to built a cardiovascular disease diagnosis system based on magnetic resonance imaging. ICA in a high-dimensional space with sparse data was applied to landmarked 3D shapes resulting from the aortic segmentation. The aortic shape variations were captured by the independent components, which were sorted using prior knowledge. The simple classification task in the 2D space spanned by the two first independent components was then performed by a simple quadratic classifier. In [41], ICA is used to perform myocardial contraction shape analysis. Here, a classification algorithm was built from the ICA components in order to automatically detect and localize abnormally contracting regions of the myocardium.

In this paper, we propose to analyze 3D images of scoliotic trunks based on ICA in order to identify progressive cases of scoliosis. The aim of this study is to determine if the deformation severity of AIS patients has increased or not (Cobb angle increase of at least 5 degrees) between successive clinical visits based on surface topography analysis, without prior knowledge from X-ray data.

The organization of the paper is as follows. In Section II, we describe the materials and the methodology used in this study. In Section III, we present the experiment results and discussion. Finally, a conclusion is given in Section IV.

II. Materials and Methods

A. Data acquisition

Over the last thirty years, several techniques have been used for non invasive evaluation of scoliosis. In this context, an optical surface digitizing system (Creaform Inc., Lévis, QC, Canada) is used at the scoliosis clinic of Sainte-Justine Hospital. The precision of the 3D reconstruction of the trunk surface using this system was evaluated by measuring the mean normal distance between the 3D reconstruction of an anthropomorphic manikin with the optical digitizers and a set of point markers on the object surface digitized with a coordinate measuring machine (CMM). This distance was evaluated at $1.1 \pm 0.9mm$ [36]. The acquisition system has four scanners (Capturor II Large Field) placed around the patient (at the back, at the front and to the right and left sides of the front angulated at about 55 degrees in order to minimize occlusion by the patient's arms). Visible markers are affixed to the patient's skin to indicate several anatomical landmarks: left and right anterior-superior iliac spines (ASIS); suprasternal notch; xiphoid process; spinous process of the prominent vertebra (C7-T1); middle of the posterior-superior iliac spines (PSIS); left and right iliac crests (lateral); left and right inferior limits of the ribcage. The patient must be centered in the field of view of the four cameras with a free-standing anatomical posture; see Figure 1. Subjects must be at the center of the system (marked on the floor) with their shoes removed and with any long hair tied up over the neck. They are asked to stand still during acquisition, focusing on a point above the front digitizer. Each scanner consists of a CCD camera and a structured light projector. The large field scanner model has a viewing volume of 1200 mm x 900 mm x 1000 mm, a lateral resolution of 1.2 mm, a depth resolution of 1.0 mm and a camera resolution of 0.8 megapixels. The Creaform body digitizer technology combines phase-shifting interferometry and active optical triangulation. Each of the four scanners provides a partial 3D surface of the trunk and the total acquisition time is slightly under 5 seconds. The vast majority of patients at the scoliosis clinic of Sainte-Justine Hospital accept full torso surface scanning; we estimate that the refusal rate is between 2% and 4%.

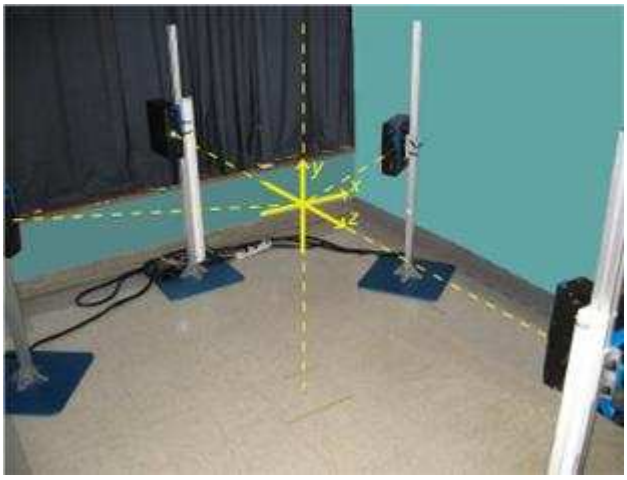

Fig. 1. Configuration of Creaform digitizers at Sainte-Justine Hospital.

B. 3D trunk reconstruction

The 3D reconstruction of the whole trunk surface of a scoliotic patient using the Creaform (*Editing and Merging*) software is not automatic. It requires manual interventions that can take considerable time (on average 20 minutes) to reconstruct the trunk surface of a single scoliotic patient. Moreover, these manual interventions result in low reproducibility. We developed an automatic method for reconstructing in 3D the trunk surface of scoliotic patients to reduce the time required to obtain each 3D trunk model. The advantage of this new, automatic and fast method is to enable the rapid construction of a large database of 3D trunk surface models of scoliotic patients in different postures as well as of non-scoliotic cases. Moreover, the results are completely reproducible. Our novel 3D trunk surface reconstruction method consists of three steps: preprocessing of the four noisy polygonal surfaces from the Creaform digitizers, registration of these polygonal surfaces and merging the geometries and textures.

Fig. 2. Merging the four polygonal surfaces.

Firstly, to remove the noise from the 3D polygonal surfaces, we propose the bilateral filter for its simplicity, speed and ability to remove noise while preserving 3D surface features [15]. The bilateral filter uses the local neighborhoods to filter vertices $\mathbf{v}$ of the mesh in the normal direction using the following equation:

$$\hat{\mathbf{v}} = \mathbf{v} + d.\mathbf{n}$$

The calculation of the displacement d along the normal $\mathbf{n}$ of each vertex $\mathbf{v}$ is given by the following equation:

$$d = \frac{\sum_{i=1}^{K}(w_c.w_s).h}{\sum_{i=1}^{K} w_c.w_s}$$

K represents the number of neighbors $\{\mathbf{q_i}\}$ of the vertex $\mathbf{v}$. w_c is the closeness smoothing filter, the standard Gaussian filter with parameter σ_c; it is given by following equation:

$$w_c = exp\Big(-\frac{\|\mathbf{v}-\mathbf{q_i}\|^2}{2\sigma_c^2}\Big)$$

$\|\mathbf{v}-\mathbf{q_i}\|$ represents the Euclidean distance between the vertex $\mathbf{v}$ and its neighbor $\mathbf{q_i}$.

w_s is the feature-preserving weight function; it is given by following equation:

$$w_s = exp\Big(-\frac{<\mathbf{n}, \mathbf{v}-\mathbf{q_i}>^2}{2\sigma_s^2}\Big)$$

$<\mathbf{n}, \mathbf{v}-\mathbf{q_i}>$ represents the dot product of the normal $\mathbf{n}$ with the vector $\mathbf{v}-\mathbf{q_i}$. This dot product represents the offset of the neighbor $\mathbf{q_i}$ to the tangent plane $P(\mathbf{v}, \mathbf{n})$ defined by the pair $(\mathbf{v}, \mathbf{n})$.

We have validated the smoothing parameters (σ_c, σ_s) by calculating the average point to point distance between the noisy surface and its filtered counterpart for 28 polygonal surfaces. Thus, we have selected the values of the smoothing parameters $\sigma_c = \sigma_s = 3$, since, qualitatively, noise is no longer visible on the filtered surface, while quantitatively the average distance calculated over the 28 polygonal surfaces is small (0.26 ± 0.33 mm), which is less than the depth resolution of the Creaform system (1 mm).

Subsequently, we introduced a measure to automatically and rapidly compute the quality of triangles and to eliminate those of poor quality while at the same time keeping a minimum percentage of triangles to obtain a good 3D reconstruction of the trunk surface. The most common measure of the quality of triangles is given by the following formula [37]:

$$\begin{aligned} q &= 2\frac{r_{in}}{r_{out}} \\ &= \frac{(b+c-a)(c+a-b)(a+b-c)}{abc} \end{aligned} \quad (1)$$

r_{in} and r_{out} represent the radii of the inscribed and circumscribed circles of the triangle respectively. The terms a, b and c represent the lengths of the sides (AB, AC, BC) of the triangle ABC. We have selected the value $q = 0.3$ for the quality factor because it eliminates triangles of poor quality while at the same time keeping a minimum percentage of triangles (40% of all triangles of the initial mesh) to obtain a good 3D reconstruction of the trunk surface. We have validated this parameter on 145 patients in different positions (standing and lateral bending).

Secondly, the data captured by each digitizer are expressed in a coordinate system related to the camera. It is therefore necessary to register all the data into a common coordinate system. Since the time required to acquire the surface of the trunk with four cameras is quite short (under five seconds), we consider that the patient does not move. Also, the operator repeats the acquisition once: if patient movement is visible in the first acquisition, the other one is used. Hence, we exploit a rigid registration technique that uses the initial registration matrices computed by the multi-head calibration

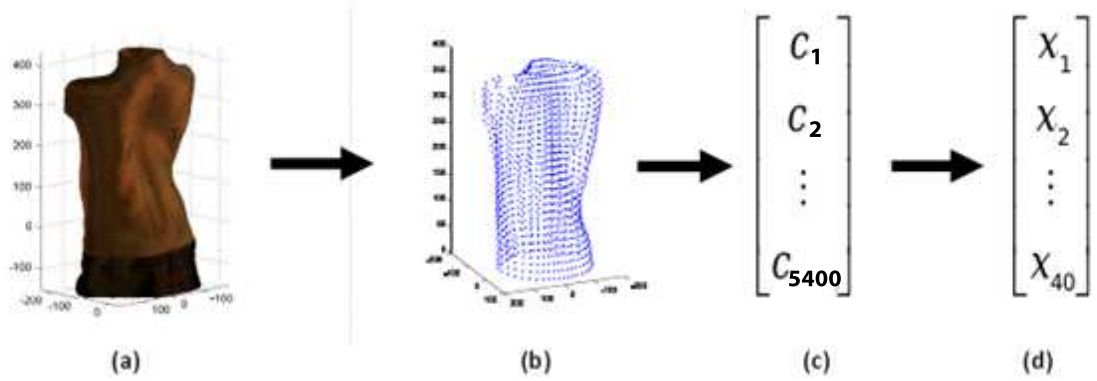

Fig. 3. Features extraction process: (a) 3D trunk image; (b) cloud of 1800 points; (c) vector of 5400 components; (d) 40 components resulting from PCA.

of the Creaform system. The rigid registration consists in transforming each point $p(x, y, z) \in \mathbb{R}^3$ belonging to each polygonal surface into a point $q(x^{'}, y^{'}, z^{'}) \in \mathbb{R}^3$ using the following equation:

$$q = \mathbf{R}p + \mathbf{T} \tag{2}$$

$\mathbf{R}$ represents the rotation matrix and $\mathbf{T}$ represents the translation matrix.

The rigid registration is followed by a refinement step using the ICP (Iterative Closest Point) algorithm to correct errors. The aim of the ICP algorithm is to iteratively register two point clouds that partially overlap into a common coordinate system based on an initial estimate of the transformation [7]. The steps performed iteratively until convergence are as follows:

- match all the points ($\{p_i\},\ i = 1 : N$) belonging to the source surface (right or left side of patient) with all the points ($\{q_i\},\ i = 1 : N$) belonging to the destination surface (front of patient);
- estimate the rigid transformation (translation and rotation) that minimizes the mean squared errors between the corresponding points ($\{p_i\}$ et $\{q_i\}$):

$$\mathbf{E} = \frac{1}{N}\sum_{i=1}^{N} |\mathbf{R}p_i + \mathbf{T} - q_i|^2 \tag{3}$$

- transform the points ($\{p_i\},\ i = 1 : N$) using the estimated transformation to align them with the points ($\{q_i\},\ i = 1 : N$).

Thirdly, after the filtering and registration steps, we propose a method for merging the four polygonal surfaces (see figure 2) based on the Poisson equation [29]. The Poisson surface reconstruction is a hybrid method, being both global and local. It is global since it considers all points at once, and local since it is based on a hierarchical set of basis functions with compact support, which reduces the Poisson equation to a sparse linear system. This method generates a closed and smooth surface and the resulting mesh contains around 70,000 vertices (for an average patient trunk) with no duplicate vertices nor intersecting polygons.

Finally, the texture information associated to the partial surfaces must also be merged. Indeed, the Poisson surface reconstruction only allows merging of the geometry of the four polygonal surfaces. However, the texture of the 3D trunk reconstruction is needed to detect the positions of markers affixed to the patient's skin and other anatomical landmarks. To merge the textures, we orthogonally project the merged polygonal surface onto the six faces of a cube according to the orientations of the normal vectors of the mesh triangles. Then, we similarly project the four textures of each face on the six faces of the cube, we save the texture obtained and for those triangles that were created by the geometries merge step, we interpolate their texture by averaging all the colors on all four faces.

C. Features extraction

First of all, several preprocessing steps are performed before applying ICA. The training trunk models are aligned in order to remove unwanted variations. For this task, we use Generalized Procrustes alignment [18], in which registration is done using isomorphic scaling, translation, and rotation.

Before the alignment step, each scoliotic trunk 3D image is decomposed into 1800 points (30 sections and 60 points per section) and after the alignment, the feature vector is built from the 3D coordinates (x, y, z) of each point. Thus, each torso is represented by a vector whose length is $5400 = 1800 \times 3$. The optimal numbers of sections and points per section are obtained manually after using a grid method through cross-validation procedure.

In general, analyzing an object based on statistical methods with a large number of features is not recommended because working in high-dimensional space entails the well-known "curse of dimensionality" problem. To avoid this, we use Principal Component Analysis (PCA) to reduce the dimensionality of the data. PCA is a mathematical technique that uses an orthogonal transformation to convert a number of (possibly) correlated variables into a (smaller) number

of uncorrelated variables. However, PCA focuses on the components that provide large variations in the data and hasn't the capacity to preserve the smaller variability. Thus, we select 40 components that provide virtually all of the total variance (99%). Figure 3 illustrates each step of the features extraction process from 3D image to feature vector with 40 components.

D. ICA modeling

Let us consider a dataset $\mathcal{D}$ comprising ℓ samples $\{x_1, \ldots, x_\ell\}$ with $x_i \in \mathbb{R}^d$. ICA attempts to find a linear transformation :

$$X = As \tag{4}$$

where the statistical independence between the variables $s = (s_1, \ldots, s_n)$ is maximized. The random variables s are called *independent components* (ICs), with $s_i \in \mathbb{R}^d$ and $A \in \mathbb{R}^{\ell \times n}$ is a *mixing matrix*.

Thus, each sample x_i of dataset $\mathcal{D}$ is represented by summing the independent components weighted by the elements of the mixing matrix A:

$$x_i = \sum_{k=1}^{n} A_{ik} s_k \tag{5}$$

The previous equation is a common definition of ICA. However, it is not possible in the general case to find a linear transformation that gives strictly independent components. Thus, in practice, some assumption is made on the data and a specific definition is used for the function that measures independence.

The following fundamental restrictions (in addition to the basic assumption of statistical independence) are imposed in order to ensure the identifiability of the ICA model [26]:
a) All the independent components s_i, with the possible exception of one, must be non-Gaussian.
b) The number of observed data ℓ must be at least as large as the number of independent components n, i.e., $\ell \geq n$.
c) The matrix $\mathbf{A}$ must be of full column rank.

Statistical independence is the key in all the algorithms designed to perform ICA. Usually, an objective function measuring independence is chosen and optimized. In the literature, we found various methods based on different objective functions, such as measuring of non-Gaussianity (principle used by the FastICA algorithm [25]), minimization of mutual information [6] or maximum likelihood estimation [9]. Maximum likelihood estimation is a popular approach for estimating the ICA model. This technique is also connected to the infomax principle and it is shown in [34] that this method is essentially equivalent to minimization of mutual information.

In this study, ICA is applied to training data using the FastICA algorithm [25]. The independent components $s = (s_1, \ldots, s_n)$ and the projection of the training data (mixing matrix A) into the ICA space are estimated by maximizing the statistical independence. The FastICA algorithm uses a fixed-point iteration technique that provides an accurate solution and fast convergence. It is 10-100 times faster than other ICA algorithms, which are based on conventional gradient descent methods.

Let us suppose that we have two 3D scoliotic trunk images acquired at different times for the same subject. The comparison between their weight vectors A_i provides information on the scoliosis progression. The comparison is performed by calculating the L1 norm distance between the weight vectors. Thus, a progression of the scoliotic deformity is detected if this distance is superior to a threshold α_0 fixed in advance during the ICs selection. The overview of the proposed system is shown in Figure 4.

E. Independent components selection

Unlike PCA, where the components are ordered based on the rate of variance retained, most ICA algorithms provide the ICs in arbitrary order, thus making it more difficult to exploit their results. Thus, in literature, various techniques are proposed. Hyvarinen et al. [24] exploit the residual dependence structure in order to define a topographic order or the components, and therefore the result is used to sort the ICs. In [20], the ICs are sorted based on their data power, representing the amount of input data variance explained by each IC. This technique resembles the eigenvalues used to perform component selection in PCA. But in practice, this technique is not suitable because an important aim of ICA is to detect local (small) variations. Cheung et al. [10, 11] have proposed to order the ICs by using a reconstruction error such as Mean Square Error (MSE) or Relative Hamming Distance (RHD) function. They give a strategy to determine a sub-optimal ordering based on a Testing-and-Acceptance (TnA) algorithm that uses a reconstruction error function. The TnA method gives good results, but a major issue of this technique concerns the number of ICs to keep. I.e., how many ICs should be selected after the ordering step? Thus, these previous methods are not appropriate since our specific problem requires ICs selection and α_0 optimization.

A combinatorial approach can be appropriate for the ICs selection problem; in our case, we decided to use a Genetic Algorithm (GA) [21, 22], which works very well on combinatorial problems. The GA is a particular case of Evolutionary Algorithms that are based on biological phenomena [4]. Specifically, the GA imitates the operations produced during the reproduction of a living species. The GA, unlike classical optimization methods, does a parallel search and it has the advantage of adapting to complex problems in which differentiability and convexity are not guaranteed. Also, continuity of the search space is not a constraint for the GA. Figure 5 provides a flowchart representation of the GA process.

In this work, the following optimization problem is considered to select both the ICs and the value of α_0:

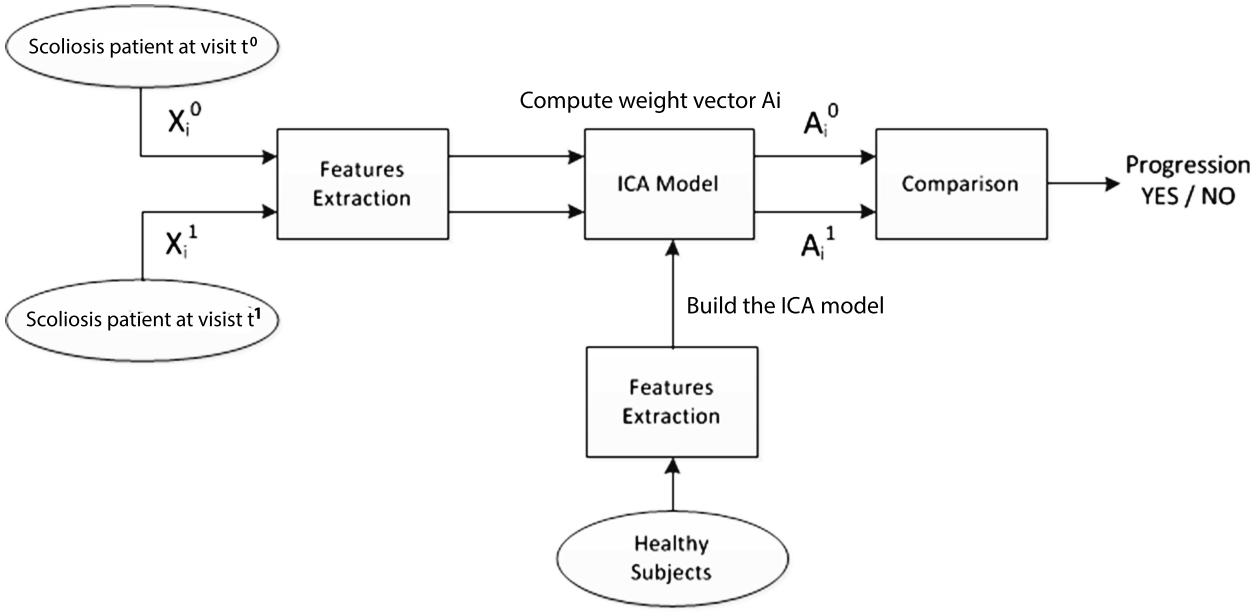

Fig. 4. Global overview of the proposed system.

$$\max_{s_P,\alpha_0} f(s_P,\alpha_0)$$
$$\text{subject to:}$$
$$g(s_P,\alpha_0) \geq 0.95 \quad (6)$$

where s_P represent the selected ICs,

$$\begin{aligned} f(s_P,\alpha_0) &= specificity \\ &= \frac{\text{number of true negatives}}{\text{number of (true negatives+ false positives)}} \\ g(s_P,\alpha_0) &= sensitivity \\ &= \frac{\text{number of true positives}}{\text{number of (true positives+ false negatives)}} \end{aligned}$$

with the following notations:
- True positive: scoliosis has progressed and is correctly identified as progressive;
- False positive: scoliosis has not progressed and is incorrectly identified as progressive;
- True negative: scoliosis has not progressed and is correctly identified as non-progressive;
- False negative: scoliosis has progressed and is incorrectly identified as non-progressive.

1) Representation: Our goal is to find an optimal subset of p ICs taken from the pull of the n ICs obtained after running the ICA algorithm. Thus, each solution is represented in the genetic domain by a chromosome with n genes, as an array of n bits. In this study, we use a binary representation where bit 1 means a given IC is selected and bit 0 means the IC is unselected. For example, if we have a problem with 7 initial ICs, an individual solution of the population can be represented by $(1;0;0;1;1;0;0)$ if only (s_1, s_4, s_5) are selected, or $(0;1;0;1;0;1;1)$ if only (s_2, s_4, s_6, s_7) are selected.

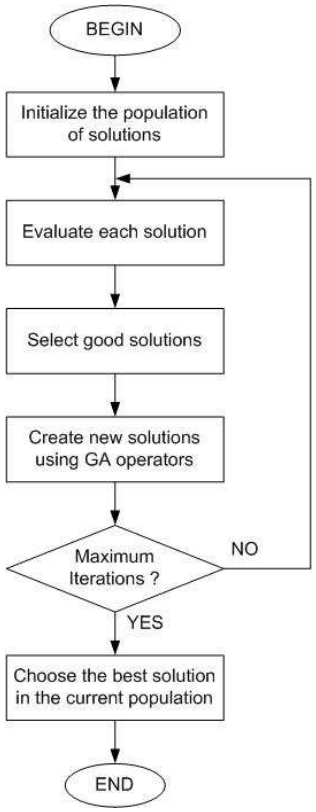

Fig. 5. Genetic algorithm process

2) Evaluation: This step of the GA is necessary in order to determine the quality of each candidate solution in the population. In this case, we compute the value of the objective function defined by $f(s_P,\alpha_0)$ under the constraint $g(s_P,\alpha_0) \geq 0.95$. In practice, we first determine the value of the threshold α_0 yielding a sensitivity of 95%, and the function $f(s_P,\alpha_0)$ is then calculated.

3) Selection: The selection operator performs the following tasks: identify good solutions in a population, make multiple copies of the good solutions and eliminate bad solutions from the population. There are several techniques for carrying out this selection task; for our problem, we have chosen a method called *Tournament selection* [3, 17], which has several advantages: it is efficient to code, works on parallel architectures and allows the selection pressure to be easily adjusted. In addition, we use a heuristic that enables us to select the best solution at each iteration (generation). This is because, when we use the Tournament selection technique, we do not have any guarantee that the best solution has been selected at that moment. Hence, we first select the best solution in the current population at each generation and, second, we complete the selection using the Tournament technique.

4) Crossover: The crossover operator is one of the two GA operators that create new solutions in the population. Crossover is the process of combining the genes of one individual with those of another to create new individuals that inherit characteristics from both parents. As with the selection operator, there are a number of crossover operators in the GA literature [39]. For this study, we use the three-points crossover technique, where each old individual is divided into four parts (at three points) and the new individual is build by randomly choosing the successive parts from its parents. In figure 6, an example of the three-points crossover technique is illustrated.

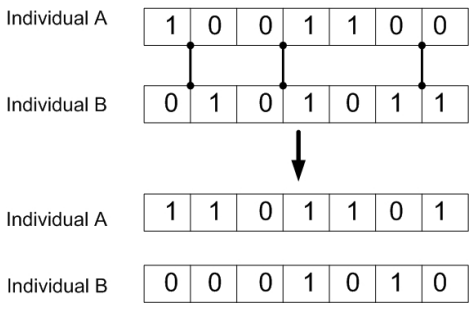

Fig. 6. Example of the crossover operator. Two individuals (solutions) are shown before and after the three-points crossover technique has been applied.

5) Mutation: In general, when the mutation operator is applied to a chromosome (individual), a randomly selected gene is changed into its opposite. A new individual is thus created in the population. When a bit 0 is changed into 1 at the $j-th$ position, this means that the corresponding component s_j is selected in the new solution, whereas the mutation from bit 1 to 0 means s_j is deselected.

F. Validation

The validation cohort for this study is composed of fifty-eight subjects whose data were collected between 2010 and 2012. The subjects fall into two groups: healthy subjects and AIS patients. The first group includes 28 healthy subjects who came to the scoliosis clinic because of their trunk appearance but received a negative diagnosis based on clinical and X-ray exams. The second group consists of 30 AIS patients who each had three clinical visits (with trunk surface acquisitions) in the 2010-2012 period. The inclusion criteria for our cohort were the following: 1) diagnosis of AIS, 2) age between 10 and 18 years when the acquisitions were taken and 3) Cobb angle measurement of the main curve greater than 10 degrees. We excluded from this study patients who had previous spinal surgery or who were undergoing brace treatment. Table 1 reports the maximum and mean Cobb angle values measured in the thoracic (T), thoraco-lumbar (TL) and lumbar (L) spinal regions for the three visits, for the second group (scoliosis group).

TABLE I
VARIATION OF COBB ANGLE IN DEGREES WITHIN SCOLIOSIS GROUP FROM FIRST VISIT TO THIRD VISIT

	Visit 1			Visit 2			Visit 3		
	T	TL	L	T	TL	L	T	TL	L
Mean value	30	24	27	34	26	31	36	28	31
Maximum value	47	30	49	58	38	49	59	41	51

To establish whether a patient's scoliosis has progressed or not between two successive visits, we look at the Cobb angles in the three spinal regions: the scoliosis is labeled as progressive if at least one of the three measurements increases by 5 degrees or more. Thus, for the same subject, we can observe progression between visits 1 and 2 and stability between visits 2 and 3, as seen in the example provided in Table II. This labelling is considered as the ground truth in this study.

TABLE II
EXAMPLE OF COBB ANGLE VARIATION FROM FIRST VISIT TO THIRD VISIT

	Visit 1			Visit 2			Visit 3		
	T	TL	L	T	TL	L	T	TL	L
Cobb angles	45	< 10	43	54	< 10	45	54	< 10	46
	Progression between visits 1 and 2								
				Stability between visits 2 and 3					

The kernel of the detection system is obtained using the data from the healthy subjects. The FastICA algorithm is run on the 28 healthy samples to construct the ICA model; the progression detection system is then tested on the scoliotic patients. The scoliosis test set contains 90 samples corresponding to the 30 patients whose data were collected at three clinical visits each. For the progression/non-progression labellings between pairs of successive visits, we have 60

TABLE III
MEAN VALUE OF COBB ANGLE WITHIN PROGRESSIVE GROUP AND NON-PROGRESSIVE GROUP FROM FIRST VISIT TO THIRD VISIT

	Visit 1	Visit 2	Visit 3
Progressive group	31	38	44
Non-progressive group	29	30	30

cases in all, consisting of 26 progressive cases and 34 non-progressive cases. Table III gives the mean value of Cobb angle within progressive group and non-progressive group from first visit to third visit. Between two visits, 3D trunk images of a given patient are analyzed using the proposed system to obtain the progression result. To evaluate the performance of our system, the progression results thus obtained are compared to the ground truth labels based on the Cobb angle variations.

Considering the relatively small size of the scoliosis group, it is not advisable to reduce this set further by forming a separate validation set in order to set the value of α_0 and select the ICs. Therefore, we choose "leave-one-out" cross-validation (LOOCV) to estimate the performance of our classification system. The LOOCV procedure is a good technique for evaluating classifier generalization performance, the idea being to test the generalization capacity of the classifier through unseen data. LOOCV is almost unbiased and its error should be relatively informative about the generalization error of the classifier (see [33, 44]).

III. EXPERIMENTAL RESULTS AND DISCUSSION

The first stage of ICA modeling, namely computing the ICs, used the group of healthy subjects. We ran the FastICA algorithm on the 28 healthy samples and obtained 27 independent components sorted by the genetic algorithm. As described in section II-F above, a LOOCV procedure is used in order to set the parameters (s_P, α_0) and to test the system on different subsets from the scoliosis group. Table IV summarizes the results obtained using this evaluation procedure.

TABLE IV
RESULTS OF SCOLIOSIS PROGRESSION DETECTION

	Labelling using radiographs (ground truth)	
	Progressive cases	Non-progressive cases
Detected as progressive	24	7
Detected as non-progressive	2	27
	26	34

The proposed system detected 24 out of 26 real cases of progression, which represents 93%, and 27 out of 34 real cases of non-progression, which represents 80%. In order word, the sensitivity of our system is 93% and the specificity is 80%. Conversely, only 7% of scoliosis progressions are not detected while 20% of non-progressive cases are determined as having progressed.

In fact, we set the decision threshold low in order to obtain a better accuracy among positive samples; indeed, it is better from a clinical standpoint to minimize false negatives than false positives. When we analyze the two undetected progression cases, we remark that both patients in question have double major spinal curves; the effect of that type of scoliosis on external deformity tends to "balance out" between the thoracic and lumbar regions. Therefore, detecting scoliosis progression based solely on trunk shape analysis becomes more difficult in such cases.

We can conclude from the very low false negative rate (0.07) that our approach is efficient at detecting the patients whose scoliosis progresses. This result confirm that the progression of the spinal curve also affects the appearance of the patient's trunk and that an appropriate computing system is able to detect the evolution of the trunk deformity.

Previous studies that attempted to estimate internal Cobb angles from external trunk shape met with limited results. That is in fact a very difficult problem because the mechanical characteristics of the soft tissues are different for each patient. Thus, the same scoliosis severity (same Cobb angle) will not necessarily produce the same external deformity in two different subjects. However, when the analysis and comparison are done on the same subject between clinical visits, the biomechanical variables affecting the relationship between internal and external shapes can be considered constant under certain conditions. In the present study, each patient is compared only to him/herself over time, and the above-mentioned problems relating to inter-patient variability are thus avoided. Unlike previous studies that focused on the predictive factors for the Cobb angle or others spinal indices, this is the first time that a quantitative comparison between external geometries of the scoliotic trunk has been performed over time.

Moreover, at the heart of our study is the use of ICA. This statistical tool is able to capture local shape variations. Unlike other statistical techniques, ICA does not assume that the data distribution is normal, nor does it focus only on the large variations in the data. Thus, shape analysis with ICA preserves the small scale variability without assuming Gaussianity. In this work, 3D image analysis of scoliotic trunks based on ICA makes possible the automatic monitoring of scoliosis progression by providing a framework in which a small variation in a patient's trunk shape (due to an increase in Cobb angle of at least 5 degrees) is detectable. The complete process from scanning to detection takes about 10 minutes.

As for the clinical relevance of this study, our system could

be used for screening purposes. During the scoliosis clinical follow-up, the physician could use the proposed approach to determine whether a given patient's scoliosis has progressed or not. Subsequently, an X-ray examination would be used to confirm the trunk surface-based diagnosis only if progression is detected by the screening system. Functioning in this way, most patients with non-progressive scoliosis would be spared unnecessary X-ray exams. Thus, our non-invasive system could be used in order to prevent cumulative radiation exposure in many cases. According to our experimental results, in 27 out of 34 cases of non-progression between two visits, the patient would not have to undergo an X-ray exam and its consequences.

IV. Conclusion

In this work, we have presented a computer-aided diagnosis (CAD) system that is able to identify progressive cases of scoliosis using 3D trunk images obtained from a non invasive surface acquisition setup. The CAD system is designed using ICA, which constitutes an innovation of this study. Also, we have presented a novel method for selecting relevant ICs based on a genetic algorithm. To our knowledge, this is the first time that ICA has been used to perform scoliotic trunk analysis.

Moreover, the results demonstrate the clinical usefulness of the proposed system for scoliosis follow-up. In future, we aim to build a system to predict scoliosis progression based on surface topography and ICA. In this work, the challenge will lie in how to estimate the evolution of the trunk deformity at a future point in time based on past observations. We expect to develop this new system by incorporating time series analysis in the ICA procedure.

Acknowledgments

The authors would like to thank Marjolaine Roy-Beaudry of SJUHC for her technical support during data collection and Philippe Debanne for revising this manuscript. They would also like to thank the Groupe de Recherche en Sciences et Technologies Biomedicales (GRSTB) of the Fonds de recherche en sante du Quebec (FRSQ) and the MENTOR program of the Canadian Institutes of Health Research (CIHR) for their financial support.

References

[1] Mathias M. Adankon, Hubert Labelle, Jean Dansereau, and Farida Cheriet. Analysis of scoliosis trunk deformities using ica. In *IEEE SSPA 2012*, 2012.

[2] P.O. Ajemba, N.G. Durdle, and V.J. Raso. Characterizing torso shape deformity in scoliosis using structured splines models. *Biomedical Engineering, IEEE Transactions on*, 56(6):1652 –1662, june 2009.

[3] Thomas Back. *Evolutionary Algorithms in Theory and Practice: Evolution Strategies, Evolutionary Programming, Genetic Algorithms*. New York, Oxford Univ. Press, 1996.

[4] Thomas Back, Ulrich Hammel, and Hans paul Schwefel. Evolutionary computation: Comments on the history and current state. *IEEE Transactions on Evolutionary Computation*, 1:3–17, 1997.

[5] K. Bae, S. Noh, and J. Kim. Iris feature extraction using independent component analysis. In *Audio-and Video-Based Biometric Person Authentication*, pages 1059–1060. Springer, 2003.

[6] A.J. Bell and T.J. Sejnowski. An information-maximization approach to blind separation and blind deconvolution. *Neural computation*, 7(6):1129–1159, 1995.

[7] P.J. Besl and N.D. McKay. A method for registration of 3-d shapes. *IEEE Transactions on pattern analysis and machine intelligence*, 14(2):239–256, 1992.

[8] L. Boquete, S. Ortega, J.M. Miguel-Jiménez, J.M. Rodríguez-Ascariz, and R. Blanco. Automated detection of breast cancer in thermal infrared images, based on independent component analysis. *Journal of Medical Systems*, pages 1–9, 2010.

[9] J.F. Cardoso. High-order contrasts for independent component analysis. *Neural computation*, 11(1):157–192, 1999.

[10] Y. Cheung and L. Xu. Independent component ordering in ica time series analysis* 1. *Neurocomputing*, 41(1-4):145–152, 2001.

[11] Yiu-Ming Cheung and Lei Xu. An empirical method to select dominant independent components in ica for time series analysis. In *Neural Networks, 1999. IJCNN '99. International Joint Conference on*, volume 6, pages 3883 –3887, jul 1999.

[12] P Comon. Independent component analysis, a new concept ? *Signal Processing, Elsevier*, 36(3):287–314, 1994.

[13] M. De Seze and G. De Korvin. Can scoliosis follow up by surface topography (biomod-l®) securely predict cobb angle progression? longitudnal study; preliminary results on 60 patients. *Scoliosis*, 7(Suppl 1):O20, 2012.

[14] M. M. Doody, J. E. Lonstein, M. Stovall, D. G. Hacker, N. Luckyanov, and C. E. Land. Breast cancer mortality after diagnostic radiography - findings from the us scoliosis cohort study. *Spine*, 25(16):2052–2063, Aug 2000.

[15] S. Fleishman, I. Drori, and D. Cohen-Or. Bilateral mesh denoising. In *ACM Transactions on Graphics (TOG)*, volume 22, pages 950–953. ACM, 2003.

[16] C.J. Goldberg, M. Kaliszer, D.P. Moore, E.E. Fogarty, and F.E. Dowling. Surface topography, cobb angles, and cosmetic change in scoliosis. *Spine*, 26(4):E55, 2001.

[17] D.E. Goldberg. *Genetic Algorithms in Search, Optimization and Machine Learning*. Addison-Wesley, Massachusetts, 1989.

[18] J.C. Gower. Generalized procrustes analysis. *Psychometrika*, 40(1):33–51, 1975.

[19] Michael Hansen, Fei Zhao, Honghai Zhang, Nicholas Walker, Andreas Wahle, Thomas Scholz, and Milan Sonka. Detection of connective tissue disorders from 3d aortic mr images using independent component analysis. In Reinhard Beichel and Milan Sonka, editors, *Computer*

Vision Approaches to Medical Image Analysis, volume 4241 of *Lecture Notes in Computer Science*, pages 13–24. Springer Berlin / Heidelberg, 2006.

[20] A.J. Hendrikse, R.N.J. Veldhuis, and L.J. Spreeuwers. Component ordering in independent component analysis based on data power. In R.N.J. Veldhuis and H.S. Cronie, editors, *Proceedings of the 28th Symposium on Information Theory in the Benelux*, pages 211–218, Eindhoven, June 2007. Werkgemeenschap voor Informatie- en Communicatietechniek.

[21] J. H. Holland. *Adaptation in Natural and Artificial Systems: An Introductory Analysis with Applications to Biology, Control, and Artificial Intelligence.* University of Michigan Press, 1975.

[22] J. H. Holland. *Adaptation in Natural and Artificial Systems: An Introductory Analysis with Applications to Biology, Control, and Artificial Intelligence, 2nd ed.* Cambridge, MA: MIT Press, 1992.

[23] P.O. Hoyer and A. Hyvärinen. Independent component analysis applied to feature extraction from colour and stereo images. *Network: Computation in Neural Systems*, 11(3):191–210, 2000.

[24] A. Hyvarinen, P.O. Hoyer, and M. Inki. Topographic independent component analysis. *Neural Computation*, 13(7):1527–1558, 2001.

[25] A. Hyvarinen, J. Karhunen, and E. Oja. *Independent component analysis*, volume 26. Wiley-Interscience, 2001.

[26] A. Hyvrinen. Survey on independent component analysis. *Neural Computing Surveys*, 2(4):94–128, 1999.

[27] J L Jaremko, P Poncet, J Ronsky, J Harder, J Dansereau, H Labelle, and R F Zernicke. Estimation of spinal deformity in scoliosis from torso surface cross sections. *Spine (Phila Pa 1976)*, 26(14):1583–1591, 2001.

[28] Jacob L. Jaremko, Philippe Poncet, Janet Ronsky, James Harder, Jean Dansereau, Hubert Labelle, and Ronald F. Zernicke. Indices of torso asymmetry related to spinal deformity in scoliosis. *Clinical Biomechanics*, 17(8):559 – 568, 2002.

[29] M. Kazhdan, M. Bolitho, and H. Hoppe. Poisson surface reconstruction. In *Proceedings of the fourth Eurographics symposium on Geometry processing*, pages 61–70. Eurographics Association, 2006.

[30] J. Koikkalainen and J. Lotjonen. Image segmentation with the combination of the pca- and ica-based modes of shape variation. In *Biomedical Imaging: Nano to Macro, 2004. IEEE International Symposium on*, pages 149 – 152 Vol. 1, april 2004.

[31] J.H. Lee, H.Y. Jung, T.W. Lee, and S.Y. Lee. Speech feature extraction using independent component analysis. In *Acoustics, Speech, and Signal Processing, 2000. ICASSP'00. Proceedings. 2000 IEEE International Conference on*, volume 3, pages 1631–1634. Ieee, 2000.

[32] X.C. Liu, J.G. Thometz, R.M. Lyon, and J. Klein. Functional classification of patients with idiopathic scoliosis assessed by the quantec system: a discriminant functional analysis to determine patient curve magnitude. *Spine*, 26(11):1274–1278, 2001.

[33] A. Luntz and V. Brailovsky. *On estimation of characters obtained in statistical procedure of recognition*. Technicheskaya Kibernetica, 1969.

[34] E. Oja and A. Hyvarinen. Independent component analysis: algorithms and applications. *Neural Network*, 13:411–430, 2000.

[35] EC Parent, S. Damaraju, DL Hill, E. Lou, and D. Smetaniuk. Identifying the best surface topography parameters for detecting idiopathic scoliosis curve progression. *Studies in health technology and informatics*, 158:78, 2010.

[36] V. Pazos, F. Cheriet, L. Song, H. Labelle, and J. Dansereau. Accuracy assessment of human trunk surface 3d reconstructions from an optical digitising system. *Medical and Biological Engineering and Computing*, 43(1):11–15, 2005.

[37] P.O. Persson and G. Strang. A simple mesh generator in matlab. *SIAM review*, pages 329–345, 2004.

[38] L. Seoud, J. Dansereau, H. Labelle, and F. Cheriet. Multilevel analysis of trunk surface measurements for noninvasive assessment of scoliosis deformities. *Spine*, 37(17):E1045–E1053, 2012.

[39] W. M. Spears. *The role of Mutation and Recombinaison in Evolutionary Algorithms*. Ph.D. Thesis, Fairfax, VA: George Mason University, 1998.

[40] I. A. Stokes and M. S. Moreland. Concordance of back surface asymmetry and spine shape in idiopathic scoliosis. *Spine (Phila Pa 1976)*, 14(1):73–78, Jan 1989.

[41] A. Suinesiaputra, A.F. Frangi, T. Kaandorp, H.J. Lamb, J.J. Bax, J. Reiber, and B. Lelieveldt. Automated detection of regional wall motion abnormalities based on a statistical model applied to multislice short-axis cardiac mr images. *Medical Imaging, IEEE Transactions on*, 28(4):595 –607, april 2009.

[42] N. Suzuki, G. W. D. Armstrong, and J. Armstrong. Application of moiré topography to spinal deformity. *Moreland, M. S., Pope, M. H., and Armstrong, G. W. D. (Eds): Moiré fringe topography and spinal deformity*, pages 225–240, 1981.

[43] T.N. Theologis, J.C.T. Fairbank, A.R. Turner-Smith, and T. Pantazopoulos. Early detection of progression in adolescent idiopathic scoliosis by measurement of changes in back shape with the integrated shape imaging system scanner. *Spine*, 22(11):1223, 1997.

[44] V. Vapnik and O. Chapelle. Bounds on error expectation for support vector machines. *Neural Computation*, 12(9):2013–2036, 2000.